mathematics

Article

A Novel Chaotic System with Only Quadratic Nonlinearities: Analysis of Dynamical Properties and Stability

Othman Abdullah Almatroud [1], Karthikeyan Rajagopal [2], Viet-Thanh Pham [3] and Giuseppe Grassi [4,*]

1 Department of Mathematics, Faculty of Science, University of Ha'il, Ha'il 2440, Saudi Arabia; o.almatroud@uoh.edu.sa
2 Centre for Nonlinear Systems, Chennai Institute of Technology, Chennai 600069, India; karthikeyan.rajagopal@citchennai.net
3 Faculty of Electrical and Electronics Engineering, Ton Duc Thang University, Ho Chi Minh City 758307, Vietnam; phamvietthanh@tdtu.edu.vn
4 Dipartimento Ingegneria Innovazione, Universitá del Salento, 73100 Lecce, Italy
* Correspondence: giuseppe.grassi@unisalento.it

Abstract: In nonlinear dynamics, there is a continuous exploration of introducing systems with evidence of chaotic behavior. The presence of nonlinearity within system equations is crucial, as it allows for the emergence of chaotic dynamics. Given that quadratic terms represent the simplest form of nonlinearity, our study focuses on introducing a novel chaotic system characterized by only quadratic nonlinearities. We conducted an extensive analysis of this system's dynamical properties, encompassing the examination of equilibrium stability, bifurcation phenomena, Lyapunov analysis, and the system's basin of attraction. Our investigations revealed the presence of eight unstable equilibria, the coexistence of symmetrical strange repeller(s), and the potential for multistability in the system.

Keywords: chaotic system; multistability; stability

MSC: 37M05; 34C28; 68P25

Citation: Almatroud, O.A.; Rajagopal, K.; Pham, V.-T.; Grassi, G. A Novel Chaotic System with Only Quadratic Nonlinearities: Analysis of Dynamical Properties and Stability. *Mathematics* **2024**, *12*, 612. https://doi.org/10.3390/math12040612

Academic Editor: Vladislav Vasilievich Lyubimov

Received: 14 January 2024
Revised: 16 February 2024
Accepted: 17 February 2024
Published: 19 February 2024

1. Introduction

The emergence of innovative chaotic systems marks a noteworthy advancement in the domain of chaos theory. Following Lorenz's discovery of a bounded non-periodic solution within a three-dimensional dynamical equation, which was initially devised for analyzing meteorological patterns [1], the concept of chaos has gained widespread acceptance as an explanatory framework for numerous real-world phenomena. Since then, a diverse range of researchers have endeavored to employ chaotic systems in elucidating various phenomena. For example, chaotic systems have found application in modeling the potential behavior of biological neurons [2,3]. Likewise, researchers have proposed numerous chaotic systems to capture the intricate dynamics of lasers [4,5]. Chaotic systems have made significant inroads into computational mathematics ever since Sprott introduced a collection of elegant three-dimensional chaotic systems [6]. This served as a catalyst for researchers to craft chaotic systems tailored to possess specific characteristics. For instance, they have developed various systems featuring a single stable equilibrium point [7,8] or no equilibria [9,10], a defined arrangement of equilibria [11,12], instances of multistability [13,14] and symmetry [15,16], hidden [17–19] and self-excited [20,21] dynamics, single [22,23] and multi-scroll [24,25] attractors, and even systems exhibiting hyperchaotic behavior [26,27]. In addition to the introduction of novel chaotic systems with unique characteristics, there has been a concerted effort in certain research endeavors to develop modified versions of existing models, each offering its own set of distinctive features and properties [28–30]. Furthermore, alongside these explorations into new and adapted chaotic systems, a parallel line of investigation has emerged delving into strategies for controlling chaos in nonlinear dynamics. On the other hand, certain investigations have pursued strategies for controlling nonlinear dynamics, such as controlling chaos synchronization [31] or special dynamical properties [32].

This paper presents a novel chaotic system characterized by only quadratic nonlinearities and investigates its dynamical properties and stability. Section 2 introduces the mathematical definition of this chaotic system, and Section 3 analyzes its dynamical properties employing tools like bifurcation diagrams, Lyapunov spectra, and the basin of attraction. Finally, Section 4 offers concluding remarks for this paper.

2. Mathematical Definition

Chaos is commonly observed in systems featuring nonlinear terms, although not in all systems with nonlinearity. This observation has spurred numerous valuable studies aimed at proposing systems capable of exhibiting chaos under specific parameter settings or initial conditions. Some proposed systems stand out for their elegance, attributed to the low dimensionality and simplicity of their nonlinear terms and/or parameter values [33]. Most chaotic systems incorporate linear and nonlinear terms [6,33], while only a few studies have identified elegant chaotic systems comprising solely nonlinear terms [21,34]. Quadratic terms represent the simplest form of nonlinearity capable of inducing chaos. Consequently, elegant systems characterized by quadratic nonlinearities, capable of exhibiting chaos independently or in coexistence with other solutions, hold particular allure in nonlinear dynamics. In this paper, we propose a three-dimensional system that exclusively consists of quadratic nonlinearities. This system can be mathematically delineated as follows:

$$\begin{aligned} \dot{x} &= a_1 y^2 - a_2 z^2, \\ \dot{y} &= b_1 x^2 - b_2 z^2, \\ \dot{z} &= c_1 y^2 + c_2 z^2 - 1, \end{aligned} \tag{1}$$

where a_1, a_2, b_1, b_2, c_1, and c_2 are the system parameters. After conducting an extensive examination involving a wide range of initial conditions and system parameter variations, it was determined that the introduced system exhibits chaotic behavior when specific values are used, specifically when $a_1 = a_2 = b_2 = c_2 = 1$, $b_1 = 2$, and $c_1 = 3$, and considering an initial condition of $(x_0, y_0, z_0) = (1, -0.5, -1)$. To ascertain that this chaotic behavior is an inherent characteristic of the system and not merely a transient phenomenon, the Lyapunov exponents (LEs) for this chaotic solution were computed using the Wolf algorithm [35], resulting in values of $(LE_1, LE_2, LE_3) = (-0.8009, 0, 0.1090)$. Figure 1a,b demonstrates the three-dimensional chaotic attractor in the $x - y - z$ space and the time series of variable x of System (1) with the specified parameter values and initial conditions. Here, the system is solved for 2000 time units.

Upon closer examination of System (1), it becomes evident that, owing to its exclusively quadratic terms, the system remains unaltered when subjected to the transformation $(x, y, z, t) \to (-x, -y, -z, -t)$. Hence, while structural symmetry cannot be identified in System (1), it is worth noting that this system displays a symmetrical strange repeller. This symmetry is established because the time-reversed system reveals a chaotic solution that exhibits symmetry with respect to the original system's strange attractor, particularly around the origin. The trajectory within the three-dimensional state space and the time series of variable x of this symmetrical strange repeller are depicted in Figure 1c,d.

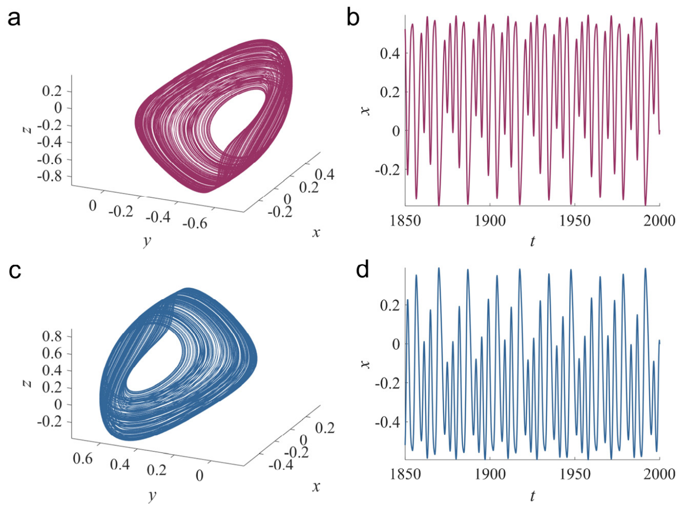

Figure 1. First row: The dynamical properties of System (1) in terms of (**a**) phase portrait in $x - y - z$ state space and (**b**) time series of the variable x. **Second row:** The dynamical properties of the time-reversed version of System (1) in terms of (**c**) phase portrait in $x - y - z$ state space and (**d**) time series of the variable x. System (1) (shown in pink) and its time-reversed version (shown in blue) are solved for the same parameters, i.e., $a_1 = a_2 = b_2 = c_2 = 1$, $b_1 = 2$, and $c_1 = 3$, while initialized with symmetric initial conditions $(x_0, y_0, z_0) = (1, -0.5, -1)$ and $(x_0, y_0, z_0) = (-1, 0.5, 1)$, respectively. After elapsing a significant transient time, the system demonstrates chaotic dynamics under the specified conditions. Moreover, it has a symmetrical strange repeller.

3. Dynamical Analysis

In this section, our objectives encompass three primary stages of dynamical analysis: assessing the stability of the system equilibria, identifying monostable and bistable regions within the parameter space via bifurcation and Lyapunov analysis, and eventually examining the system's basin of attraction.

3.1. Stability Analysis

Discovering system equilibria and conducting stability analysis are pivotal processes essential for comprehending and forecasting the behavior of intricate dynamical systems across various scientific disciplines. The equilibria can be found by setting the time derivatives (velocities) to zero. Thus, we have

$$\begin{aligned} \dot{x} = 0 \to a_1 y^2 - a_2 z^2 = 0, \\ \dot{y} = 0 \to b_1 x^2 - b_2 z^2 = 0, \\ \dot{z} = 0 \to c_1 y^2 + c_2 z^2 - 1 = 0. \end{aligned} \tag{2}$$

By solving these equations simultaneously, the equilibrium points can be found. Accordingly, System (1) is found to have eight equilibrium points:

$$\begin{aligned}
(x_1^*, y_1^*, z_1^*) &= \left(\sqrt{\tfrac{a_1 b_2}{b_1(a_1c_2+a_2c_1)}}, \sqrt{\tfrac{a_2}{a_1c_2+a_2c_1}}, \sqrt{\tfrac{a_1}{a_1c_2+a_2c_1}}\right), \\
(x_2^*, y_2^*, z_1^*) &= \left(\sqrt{\tfrac{a_1 b_2}{b_1(a_1c_2+a_2c_1)}}, \sqrt{\tfrac{a_2}{a_1c_2+a_2c_1}}, -\sqrt{\tfrac{a_1}{a_1c_2+a_2c_1}}\right), \\
(x_3^*, y_3^*, z_3^*) &= \left(\sqrt{\tfrac{a_1 b_2}{b_1(a_1c_2+a_2c_1)}}, -\sqrt{\tfrac{a_2}{a_1c_2+a_2c_1}}, \sqrt{\tfrac{a_1}{a_1c_2+a_2c_1}}\right), \\
(x_4^*, y_4^*, z_4^*) &= \left(\sqrt{\tfrac{a_1 b_2}{b_1(a_1c_2+a_2c_1)}}, -\sqrt{\tfrac{a_2}{a_1c_2+a_2c_1}}, -\sqrt{\tfrac{a_1}{a_1c_2+a_2c_1}}\right), \\
(x_5^*, y_5^*, z_5^*) &= \left(-\sqrt{\tfrac{a_1 b_2}{b_1(a_1c_2+a_2c_1)}}, \sqrt{\tfrac{a_2}{a_1c_2+a_2c_1}}, \sqrt{\tfrac{a_1}{a_1c_2+a_2c_1}}\right), \\
(x_6^*, y_6^*, z_6^*) &= \left(-\sqrt{\tfrac{a_1 b_2}{b_1(a_1c_2+a_2c_1)}}, \sqrt{\tfrac{a_2}{a_1c_2+a_2c_1}}, -\sqrt{\tfrac{a_1}{a_1c_2+a_2c_1}}\right), \\
(x_7^*, y_7^*, z_7^*) &= \left(-\sqrt{\tfrac{a_1 b_2}{b_1(a_1c_2+a_2c_1)}}, -\sqrt{\tfrac{a_2}{a_1c_2+a_2c_1}}, \sqrt{\tfrac{a_1}{a_1c_2+a_2c_1}}\right), \\
(x_8^*, y_8^*, z_8^*) &= \left(-\sqrt{\tfrac{a_1 b_2}{b_1(a_1c_2+a_2c_1)}}, -\sqrt{\tfrac{a_2}{a_1c_2+a_2c_1}}, -\sqrt{\tfrac{a_1}{a_1c_2+a_2c_1}}\right).
\end{aligned}$$

In order to assess the stability of these eight system equilibria, our initial step involves computing the Jacobian matrix for the system, as shown below:

$$J = \begin{bmatrix} \frac{\partial \dot{x}}{\partial x} & \frac{\partial \dot{x}}{\partial y} & \frac{\partial \dot{x}}{\partial z} \\ \frac{\partial \dot{y}}{\partial x} & \frac{\partial \dot{y}}{\partial y} & \frac{\partial \dot{y}}{\partial z} \\ \frac{\partial \dot{z}}{\partial x} & \frac{\partial \dot{z}}{\partial y} & \frac{\partial \dot{z}}{\partial z} \end{bmatrix} = \begin{bmatrix} 0 & 2a_1 y & -2a_2 z \\ 2b_1 x & 0 & -2b_2 z \\ 0 & 2c_1 y & 2c_2 z \end{bmatrix}. \tag{3}$$

Subsequently, in the next stage, we proceed to determine the eigenvalues of the Jacobian matrix for each equilibrium point. The eigenvalues λ_i are the solution to the characteristic equation given by $|\lambda I - J|_{(x^*, y^* z^*)} = 0$, where I is the identity matrix of the same size as J. Substituting the Jacobian matrix, we have

$$\begin{vmatrix} \lambda & 2a_1 y^* & -2a_2 z^* \\ 2b_1 x^* & \lambda & -2b_2 z^* \\ 0 & 2c_1 y^* & \lambda - 2c_2 z^* \end{vmatrix} = \lambda^3 + f_1 \lambda^2 + f_2 \lambda + f_3 = 0, \tag{4}$$

where $f_1 = -2c_2 z^*$, $f_2 = 4y^*\left(b_2 c_1 z^* - a_1 b_1 x^*\right)$, and $f_3 = 8b_1 x^* y^* z^* (a_1 c_2 + a_2 c_1)$. An equilibrium point is considered stable when all its eigenvalues possess negative real parts. Conversely, the equilibrium point is deemed unstable if at least one eigenvalue has a positive real part. Assuming $a_1 = a_2 = b_2 = c_2 = 1$, $b_1 = 2$, and $c_1 = 3$, we get

$$\begin{aligned}
\left(x_1^*, y_1^*, z_1^*\right) &\rightarrow (\lambda_1, \lambda_2, \lambda_3) = (1.2679, -1.134 \pm 1.782i), \\
\left(x_2^*, y_2^*, z_1^*\right) &\rightarrow (\lambda_1, \lambda_2, \lambda_3) = (-1.2113, 0.1056 \pm 2.1585i), \\
\left(x_3^*, y_3^*, z_3^*\right) &\rightarrow (\lambda_1, \lambda_2, \lambda_3) = (-2.52, 0.76 \pm 1.2912i), \\
\left(x_4^*, y_4^*, z_4^*\right) &\rightarrow (\lambda_1, \lambda_2, \lambda_3) = (2.1917, -1.5958 \pm 0.1852i), \\
\left(x_5^*, y_5^*, z_5^*\right) &\rightarrow (\lambda_1, \lambda_2, \lambda_3) = (-2.1917, 1.5958 \pm 0.1852i), \\
\left(x_6^*, y_6^*, z_6^*\right) &\rightarrow (\lambda_1, \lambda_2, \lambda_3) = (2.52, -0.76 \pm 1.2912i), \\
\left(x_7^*, y_7^*, z_7^*\right) &\rightarrow (\lambda_1, \lambda_2, \lambda_3) = (1.2113, -0.1056 \pm 2.1585i), \\
\left(x_8^*, y_8^*, z_8^*\right) &\rightarrow (\lambda_1, \lambda_2, \lambda_3) = (-1.2679, +1.134 \pm 1.782i).
\end{aligned}$$

As a result, under the conditions depicted in Figure 1, none of the equilibrium points exhibit stability. Furthermore, aside from their instability, it is evident that all equilibrium points yield complex conjugate eigenvalues, indicating that the system's solutions diverge from these equilibria in a spiral fashion.

3.2. Bifurcation and Lyapunov Analysis

Bifurcation analysis examines how the fundamental characteristics of a dynamic system evolve when a parameter undergoes variation. Its primary focus lies in pinpointing specific locations in the parameter space where significant qualitative shifts in the system's behavior manifest. Identifying potential multistable regions within the parameter space can be achieved by employing the forward and backward approaches to obtaining bifurcation diagrams [5,36]. In the case of flow-based dynamical systems, a common practice is to conduct bifurcation analysis by identifying the local maxima in the time evolution of the system for each specific parameter configuration. On the other hand, LE analysis is a methodology employed to numerically assess the rate at which nearby trajectories within a dynamical system either exponentially move apart or converge. This technique offers valuable insights into the system's susceptibility to initial conditions and potential for chaotic behavior.

The present study employed both forward and backward approaches for bifurcation and LEs analysis. This enabled us to unveil the system's dynamical attributes, encompassing areas of chaos and multistability within the parameter space. Figure 2 displays the forward and backward bifurcation diagrams in the left column and the LE spectra in the right column for the parameters a_2, b_1, and b_2. In each case, apart from the bifurcation parameters, the other parameter settings remained consistent with those in Figure 1. Specifically, Figure 2a illustrates the transition from a period-doubling cascade to chaos as a_2 varies within the range of $[0.85, 1.0355]$. Within this range, the system exhibits periodic solutions for $0.85 \leq a_2 < 0.912$ while for $0.912 < a_2 \leq 1.0355$, these solutions transition into chaos through a period-doubling cascade. Upon closer examination of Figure 2a, a notable expansion in the size of the attractor can be observed in the chaotic region around $a_2 \approx 0.9545$, referred to as an interior crisis. Similarly, in Figure 2c, a transition from periodic orbits to chaotic attractors occurs as the parameter b_1 changes within the range of $[1.76, 2.13]$. However, this transition occurs through a boundary crisis at $b_1 \approx 1.853$, where period-2 solutions suddenly vanish, and chaotic solutions emerge. Before and after the crisis, i.e., $1.76 \leq b_1 < 1.853$ and $1.853 < b_1 \leq 2.13$, the system has periodic and chaotic solutions, respectively. Furthermore, as depicted in Figure 2c, the system undergoes an interior crisis at $b_1 \approx 1.89$. In Figure 2e, an opposite trend is observed when b_2 varies within the range of $[0.95,\ 1.053]$. Specifically, when $0.95 \leq b_2 < 1.03898$, the system exhibits chaotic solutions. However, for higher values of b_2, i.e., $1.03898 < b_2 \leq 1.053$, the solutions become periodic following a boundary crisis at $b_2 \approx 1.03898$. Various small periodic windows can also be observed within the chaotic regions in all cases depicted in Figure 2. The associated forward and backward LE spectra corroborate all the evidence provided by the bifurcation diagrams. Furthermore, because the forward and backward diagrams overlap across the entire explored parameter region in all three cases presented in Figure 2, it can be inferred that the system is monostable under the considered settings.

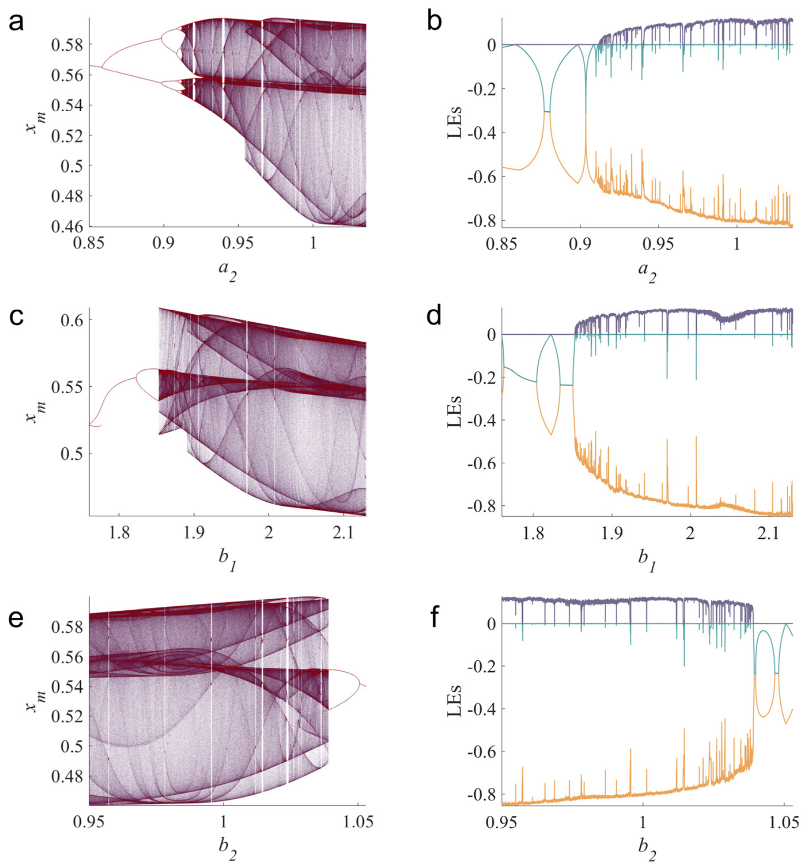

Figure 2. The dynamical characteristics of System (1) regarding the variation of the parameters (**a**,**b**) a_2 within $0.85 \leq a_1 \leq 1.0355$, (**c**,**d**) b_1 within $1.76 \leq b_1 \leq 2.13$, and (**e**,**f**) b_2 within $0.95 \leq b_2 \leq 1.053$ in terms of forward (shown in blue) and backward (shown in red) bifurcation diagrams in the left columns and forward/backward LE spectra in the right columns. Other settings are the same as in Figure 1. With the forward and backward diagrams overlapping, there is no evidence of multistability emerging from variations in the parameters.

An analogous investigation was performed on the system, with the parameters a_1, c_1, and c_2 undergoing variations within $[0.95, 2.27]$, $[1.8, 3.1]$, and $[0.96, 1.2]$, respectively, while maintaining other parameter values (except for the parameter being probed), consistent with those in Figure 1. The findings are presented in Figure 3, which illustrates the forward (blue plot) and backward (red plot) bifurcation diagrams, accompanied by the associated LE spectra. Unlike Figure 2, Figure 3 focuses on cases where the system has the potential to exhibit multistability. Specifically, as depicted in Figure 3a, when the parameter a_1 is gradually increased, a period-halving followed by a period-doubling cascade is observed. This implies that chaos is the system's solution for both low and high values of a_1 in the explored region, while intermediate values of a_1 lead to periodic solutions. However, it is only within the period-halving route, specifically within $1.208 \leq a_1 \leq 1.265$, that the discrepancy between the forward and backward diagrams is observed, indicating multistability. Furthermore, the forward diagram enters the multistable region through a period-halving bifurcation, while the backward diagram experiences an interior crisis. At the end of the multistability region, both diagrams transition into the monostable chaotic region through a boundary crisis. In Figure 3b, starting from $c_1 = 1.8$, both forward and backward bifurcation diagrams show a period-doubling cascade to chaos. However, in the chaotic region ($2.4426 \leq c_1 < 3.1$), the backward diagram presents a significant periodic window within the range of $2.59 \leq c_1 \leq 2.649$. This transition commences with a boundary crisis and proceeds into the chaotic region via a period-doubling bifurcation. In the same parameter range, the forward bifurcation depicts chaotic dynamics, entering into larger solutions through an interior crisis at $c_1 = 2.649$. Similar to Figure 3a, Figure 3c illustrates a period-halving route from periodic ($0.96 \leq c_2 < 1.071$) to chaotic ($1.071 < c_2 \leq 1.2$) dynamics. While the forward bifurcation diagram exhibits periodic dynamics within periodic windows ($1.041 \leq c_2 \leq 1.0533$), commencing with an interior crisis and concluding with a boundary crisis, the backward diagram demonstrates chaotic solutions within the same range. Like the forward diagram, the backward diagram enters the multistable region through an interior crisis and exits this region via a boundary crisis. The forward (second row) and backward (third row) LE spectra, as displayed in Figure 3, corroborate the dynamics observed in the forward and backward bifurcation diagrams presented in the first row of Figure 3. The discernible dynamical distinction, without any further analysis, indicates that when a_1, c_1, and c_2 fall within the interval $[1.208, 1.265]$, $[2.59, 2.649]$, and $[1.041, 1.0533]$, it is reasonable to anticipate the presence of at least two coexisting attractors exhibiting varying dissipation levels (as indicated by the sum of LEs).

3.3. Basin of Attraction

The term basin of attraction refers to the area within the state space of a dynamical system where initial conditions result in the system converging towards a specific solution or unbounded orbits. In simpler terms, it outlines the collection of initial states from which the system progresses toward a particular outcome, serving as evidence of the system's sensitivity to initial conditions. As revealed by Figure 3, the system has the potential to exhibit multistability. For instance, setting $a_1 = a_2 = b_2 = c_2 = 1$, $b_1 = 2$, and $c_1 = 2.6$, the system is found to have two coexisting trajectories, including a strange attractor and a period-3 orbit with $(LE_1, LE_2, LE_3) = (-0.8717, 0, 0.0874)$ and $(LE_1, LE_2, LE_3) = (-0.6231, 0.2022, 0)$, respectively. These system solutions are shown in Figure 4, considering $(x_0, y_0, z_0) = (-0.3727, -0.5, 0.2)$ and $(x_0, y_0, z_0) = (-0.3727, -0.527, 0.3)$ to obtain the chaotic (in green) and periodic (in orange) trajectories.

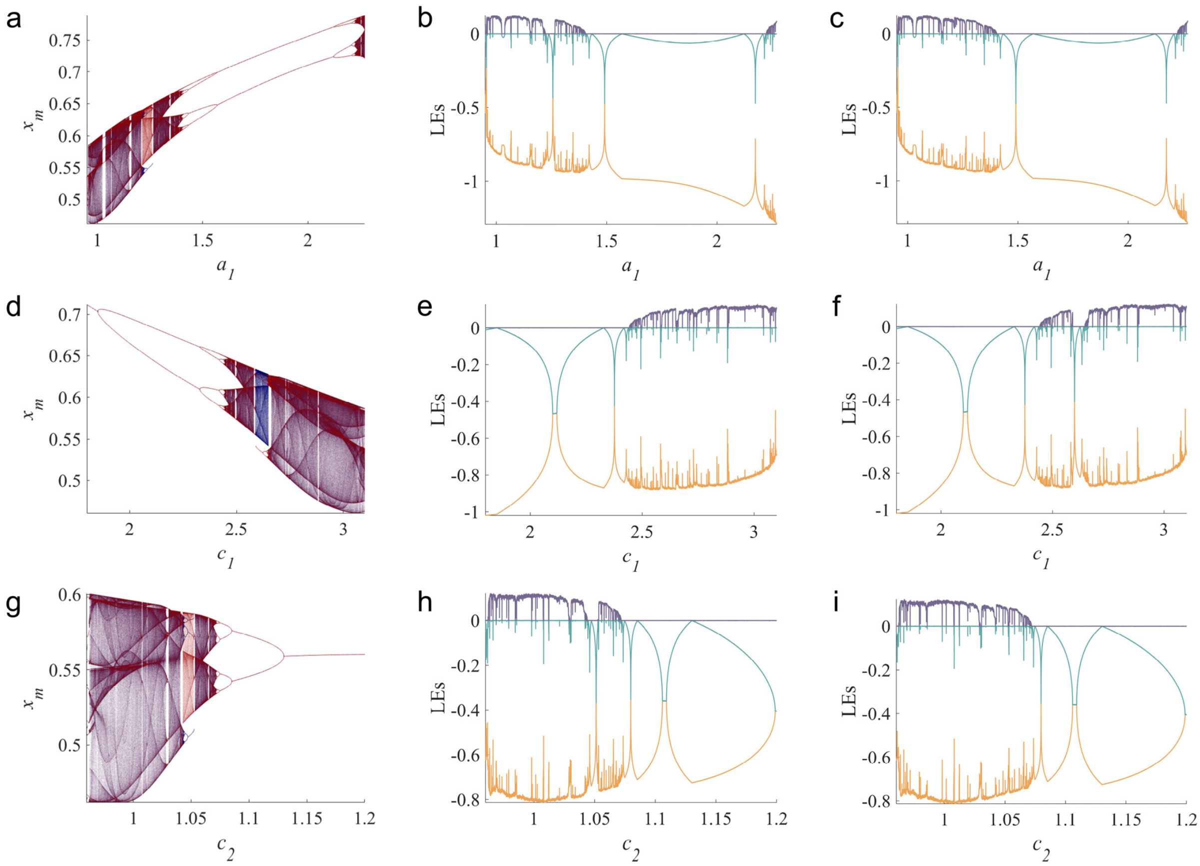

Figure 3. The dynamical characteristics of System (1) regarding the variation of the parameters a_1 (within $0.95 \leq a_1 \leq 2.27$; first column), c_1 (within $1.8 \leq c_1 \leq 3.1$; second column), and c_2 (within $0.96 \leq c_2 \leq 1.2$; third column) while $a = 2$ in terms of (**a**–**c**) forward (shown in blue) and backward (shown in red) bifurcation diagrams and (**d**–**f**) forward and (**g**–**i**) backward LE spectra. Other settings are the same as in Figure 1. In each case, the forward and backward diagrams do not exhibit congruence in specific ranges of bifurcation parameters, signifying the presence of multistability in the corresponding parameter region.

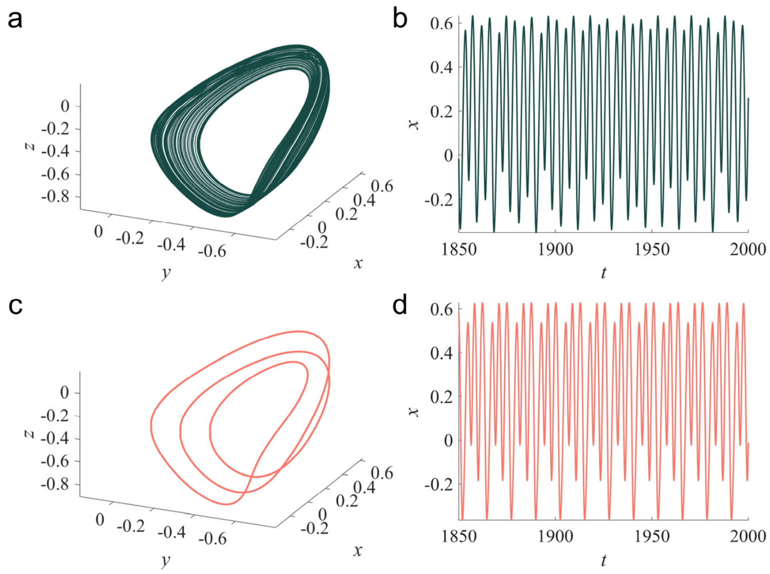

Figure 4. The dynamical properties of System (1) in terms of (**a**,**c**) phase portrait in $x - y - z$ state space and (**b**,**d**) time series of the variable x. System (1) is solved for $a_1 = a_2 = b_2 = c_2 = 1$, $b_1 = 2$,

and $c_1 = 2.6$ while initialized with the initial conditions $(x_0, y_0, z_0) = (-0.3727, -0.5, 0.2)$ and $(x_0, y_0, z_0) = (-0.3727, -0.527, 0.3)$ to obtain the chaotic (shown in green) and period-3 (shown in orange) solutions, respectively. After elapsing a significant transient time, the system demonstrates multistability, where chaotic and periodic attractors coexist.

The study of the basin of attraction for a dynamical system becomes even more interesting in the case of multistability. Hence, keeping $a_1 = a_2 = b_2 = c_2 = 1$, $b_1 = 2$, and $c_1 = 2.6$, we aimed to find the initial variable settings leading to the chaotic and periodic attractors illustrated in Figure 4. Accordingly, Figure 5 portrays six cross-sectional views of the three-dimensional $x_0 - y_0 - z_0$ state space, facilitating the recognition of the eight system equilibria. These cross sections are $x_0 = \pm\sqrt{\frac{a_1 b_2}{b_1(a_1 c_2 + a_2 c_1)}} = \pm 0.3727$ (Figure 5a,b), $y_0 = \pm\sqrt{\frac{a_2}{a_1 c_2 + a_2 c_1}} = \pm 0.527$ (Figure 5c,d), and $z_0 = \pm\sqrt{\frac{a_1}{a_1 c_2 + a_2 c_1}} = \pm 0.527$ (Figure 5e,f) planes. As portrayed in Figure 5, the system equilibria have no basin of attractions. As illustrated in Figure 5, it is evident that the system's equilibria do not possess basins of attraction. Consequently, in the parameter settings being considered, these equilibria are proven unstable without further analytical analysis. The instability of these equilibria can also be confirmed through the stability analysis described in Section 3.1, as none of the system's equilibria exhibit three negative real eigenvalues. The regions highlighted in green and orange represent the initial conditions resulting in the chaotic and periodic solutions already depicted in Figure 4. Furthermore, Figure 5 illustrates a considerable portion of unbounded orbits, signifying that the system is likely to exhibit unbounded behavior. Nevertheless, in specific regions, it can follow distinct trajectories with a bounded nature.

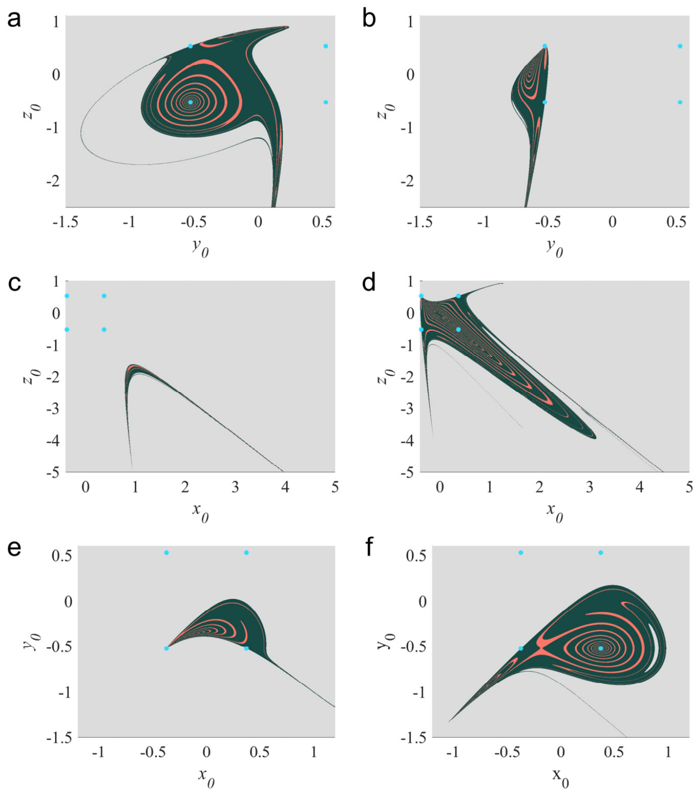

Figure 5. The sensitivity analysis through the system's basin of attraction assuming $a_1 = a_2 = b_2 = c_2 = 1$, $b_1 = 2$, and $c_1 = 2.6$ in (**a**,**b**) $x_0 = \pm 0.3727$ plane for $-1.5 \leq y_0 \leq 0.6$ and $-2.5 \leq z_0 \leq 1.1$, (**c**,**d**) $y_0 = \pm 0.527$ plane for $-0.4 \leq x_0 \leq 5$ and $-5 \leq z_0 \leq 1$, and (**e**,**f**) $z_0 = \pm 0.527$ plane for $-1.2 \leq x_0 \leq 1.2$ and $-1.5 \leq y_0 \leq 0.6$. The green dots represent trajectories converging towards the chaotic attractor in Figure 4a, while the orange dots signify convergence towards the periodic solution in Figure 4c. Gray-coded dots illustrate unbounded orbits, and the cyan color designates the system's equilibria. As these equilibria lack a basin of attraction, they are confirmed to be unstable.

It is important to note that the system was solved for each set of initial condition values to determine the basin of attraction within a predetermined parameter setting and a particular cross section. The period of the attained solution was then calculated to differentiate between periodic and chaotic dynamics.

4. Conclusions

In this paper, we introduce a novel chaotic system characterized solely by quadratic nonlinearities. We conducted an extensive analysis of its dynamical behavior employing a range of tools, such as bifurcation diagrams and LE spectra. The inherent quadratic nature of the system led to the identification of eight equilibrium points and the manifestation of repeller dynamics. Our stability analysis revealed that all equilibrium points were inherently unstable within a specific parameter configuration. Furthermore, our examination of forward and backward bifurcation analysis highlighted that the system can exhibit multistability in a distinct parameter space region. We delved into the system's basin of attraction to investigate its sensitivity to initial conditions, particularly in the multistable area. This exploration was performed while adjusting the parameters to facilitate the coexistence of a strange attractor and a period-3 solution.

Author Contributions: Conceptualization, V.-T.P.; investigation, K.R.; methodology, O.A.A.; project administration, G.G.; resources, K.R.; validation, O.A.A.; writing—original draft, V.-T.P.; writing—review and editing, G.G. All authors have read and agreed to the published version of the manuscript.

Funding: This research has been funded by the Scientific Research Deanship at the University of Ha'il, Saudi Arabia, through project number <<RG-23 087>>.

Data Availability Statement: No new data were created or analyzed in this study. Data sharing is not applicable to this article.

Conflicts of Interest: The authors declare no conflicts of interest.

References

1. Lorenz, E.N. Deterministic nonperiodic flow. *J. Atmos. Sci.* **1963**, *20*, 130–141. [CrossRef]
2. Hodgkin, A.L.; Huxley, A.F. A quantitative description of membrane current and its application to conduction and excitation in nerve. *J. Physiol.* **1952**, *117*, 500. [CrossRef]
3. Hindmarsh, J.L.; Rose, R.M.; Huxley, A.F. A model of neuronal bursting using three coupled first order differential equations. *Proc. R. Soc. B* **1997**, *221*, 87–102. [CrossRef]
4. Arecchi, F.T.; Meucci, R.; Puccioni, G.; Tredicce, J. Experimental evidence of subharmonic bifurcations, multistability, and turbulence in a Q-switched gas laser. *Phys. Rev. Lett.* **1982**, *49*, 1217–1220. [CrossRef]
5. Meucci, R.; Marc Ginoux, J.; Mehrabbeik, M.; Jafari, S.; Clinton Sprott, J. Generalized multistability and its control in a laser. *Chaos* **2022**, *32*, 083111. [CrossRef]
6. Sprott, J.C. Some simple chaotic flows. *Phys. Rev. E* **1994**, *50*, R647–R650. [CrossRef]
7. Molaie, M.; Jafari, S.; Sprott, J.C.; Golpayegani, S.M.R.H. Simple chaotic flows with one stable equilibrium. *Int. J. Bifurcat. Chaos* **2013**, *23*, 1350188. [CrossRef]
8. Wang, X.; Chen, G. A chaotic system with only one stable equilibrium. *Commun. Nonlinear Sci. Numer. Simul.* **2012**, *17*, 1264–1272. [CrossRef]
9. Jafari, S.; Sprott, J.C.; Hashemi Golpayegani, S.M.R. Elementary quadratic chaotic flows with no equilibria. *Phys. Lett. A* **2013**, *377*, 699–702. [CrossRef]
10. Nag Chowdhury, S.; Ghosh, D. Hidden attractors: A new chaotic system without equilibria. *Eur. Phys. J. Spec. Top.* **2020**, *229*, 1299–1308. [CrossRef]
11. Jafari, S.; Sprott, J.C. Simple chaotic flows with a line equilibrium. *Chaos Solitons Fractals* **2013**, *57*, 79–84. [CrossRef]
12. Barati, K.; Jafari, S.; Sprott, J.C.; Pham, V.-T. Simple chaotic flows with a curve of equilibria. *Int. J. Bifurcat. Chaos* **2016**, *26*, 1630034. [CrossRef]
13. Lai, Q.; Kuate, P.D.K.; Liu, F.; Iu, H.H.C. An extremely simple chaotic system with infinitely many coexisting attractors. *IEEE Trans. Circuits Syst. II Express Briefs* **2020**, *67*, 1129–1133. [CrossRef]
14. Chang, H.; Li, Y.; Chen, G.; Yuan, F. Extreme multistability and complex dynamics of a memristor-based chaotic system. *Int. J. Bifurcat. Chaos* **2020**, *30*, 2030019. [CrossRef]
15. Tagne, R.L.M.; Kengne, J.; Negou, A.N. Multistability and chaotic dynamics of a simple Jerk system with a smoothly tuneable symmetry and nonlinearity. *Int. J. Bifurcat. Chaos* **2019**, *7*, 476–495. [CrossRef]

16. Li, C.; Sprott, J.C.; Xing, H. Constructing chaotic systems with conditional symmetry. *Nonlinear Dyn.* **2017**, *87*, 1351–1358. [CrossRef]
17. Bao, B.C.; Bao, H.; Wang, N.; Chen, M.; Xu, Q. Hidden extreme multistability in memristive hyperchaotic system. *Chaos Solitons Fractals* **2017**, *94*, 102–111. [CrossRef]
18. Dang, X.-Y.; Li, C.-B.; Bao, B.-C.; Wu, H.-G. Complex transient dynamics of hidden attractors in a simple 4D system. *Chin. Phys. B* **2015**, *24*, 050503. [CrossRef]
19. Bao, B.; Luo, J.; Bao, H.; Chen, C.; Wu, H.; Xu, Q. A simple nonautonomous hidden chaotic system with a switchable stable node-focus. *Int. J. Bifurcat. Chaos* **2019**, *29*, 1950168. [CrossRef]
20. Ramamoorthy, R.; Jamal, S.S.; Hussain, I.; Mehrabbeik, M.; Jafari, S.; Rajagopal, K. A new circumscribed self-excited spherical strange attractor. *Complexity* **2021**, *2021*, 8068737. [CrossRef]
21. Ramesh, A.; Hussain, I.; Natiq, H.; Mehrabbeik, M.; Jafari, S.; Rajagopal, K. A new system with a self-excited fully-quadratic strange attractor and its twin strange repeller. *Int. J. Bifurcat. Chaos* **2021**, *31*, 2130047. [CrossRef]
22. Sayeed Anwar, M.; Sar, G.K.; Ray, A.; Ghosh, D. Behavioral study of a new chaotic system. *Eur. Phys. J. Spec. Top.* **2020**, *229*, 1343–1350. [CrossRef]
23. Ray, A.; Ghosh, D. Another new chaotic system: Bifurcation and chaos control. *Int. J. Bifurcat. Chaos* **2020**, *30*, 2050161. [CrossRef]
24. Wu, Y.; Wang, C.; Deng, Q. A new 3D multi-scroll chaotic system generated with three types of hidden attractors. *Eur. Phys. J. Spec. Top.* **2021**, *230*, 1863–1871. [CrossRef]
25. Liu, S.; Wei, Y.; Liu, J.; Chen, S.; Zhang, G. Multi-scroll chaotic system model and its cryptographic application. *Int. J. Bifurcat. Chaos* **2020**, *30*, 2050186. [CrossRef]
26. Joshi, M.; Ranjan, A. New simple chaotic and hyperchaotic system with an unstable node. *AEU Int. J. Electron. Commun.* **2019**, *108*, 1–9. [CrossRef]
27. Li, C.; Sprott, J.C.; Thio, W.; Zhu, H. A new piecewise linear hyperchaotic circuit. *IEEE Trans. Circuits Syst. II Express Briefs* **2014**, *61*, 977–981. [CrossRef]
28. Xu, Q.; Wang, Y.; Wu, H.; Chen, M.; Chen, B. Periodic and chaotic spiking behaviors in a simplified memristive Hodgkin-Huxley circuit. *Chaos Solitons Fractals* **2024**, *179*, 114458. [CrossRef]
29. Xu, Q.; Huang, L.; Wang, N.; Bao, H.; Wu, H.; Chen, M. Initial-offset-boosted coexisting hyperchaos in a 2D memristive Chialvo neuron map and its application in image encryption. *Nonlinear Dyn.* **2023**, *111*, 20447–20463. [CrossRef]
30. Wang, N.; Xu, D.; Iu, H.H.C.; Wang, A.; Chen, M.; Xu, Q. Dual Chua's Circuit. *IEEE Trans. Circuits Syst. I Regul. Pap.* **2023**, 1–10. [CrossRef]
31. Cao, Z.; Li, C.; Leung, M.-F. The Synchronisation Problem of Chaotic Neural Networks Based on Saturation Impulsive Control and Intermittent Control. *Mathematics* **2024**, *12*, 151. [CrossRef]
32. Chen, M.; Wang, A.; Wu, H.; Chen, B.; Xu, Q. DC-Offset Strategy for Controlling Hidden and Multistable Behaviors in Physical Circuits. *IEEE Trans. Ind. Electron.* **2023**, 1–9. [CrossRef]
33. Sprott, J.C. *Elegant Chaos: Algebraically Simple Chaotic Flows*; World Scientific: Singapore, 2010.
34. Veeman, D.; Alanezi, A.; Natiq, H.; Jafari, S.; Abd El-Latif, A.A. A Chaotic Quadratic Oscillator with Only Squared Terms: Multistability, Impulsive Control, and Circuit Design. *Symmetry* **2022**, *14*, 259. [CrossRef]
35. Wolf, A.; Swift, J.B.; Swinney, H.L.; Vastano, J.A. Determining Lyapunov exponents from a time series. *Phys. D* **1985**, *16*, 285–317. [CrossRef]
36. Sprott, J.C. A proposed standard for the publication of new chaotic systems. *Int. J. Bifurcat. Chaos* **2011**, *21*, 2391–2394. [CrossRef]